

## Optimal Control Technique for Many-Body Quantum Dynamics

Patrick Doria

*Institut für Quanteninformationsverarbeitung, Albert-Einstein-Allee 11, D-89069 Ulm, Germany  
and Politecnico di Torino, Corso Duca degli Abruzzi, 24 10129 Torino, Italy*

Tommaso Calarco and Simone Montangero\*

*Institut für Quanteninformationsverarbeitung, Albert-Einstein-Allee 11, D-89069 Ulm, Germany  
(Received 17 November 2010; published 11 May 2011)*

We present an efficient strategy for controlling a vast range of nonintegrable quantum many-body one-dimensional systems that can be merged with state-of-the-art tensor network simulation methods such as the density matrix renormalization group. To demonstrate its potential, we employ it to solve a major issue in current optical-lattice physics with ultracold atoms: we show how to reduce by about 2 orders of magnitude the time needed to bring a superfluid gas into a Mott insulator state, while suppressing defects by more than 1 order of magnitude as compared to current experiments [T. Stöferle *et al.*, *Phys. Rev. Lett.* **92**, 130403 (2004)]. Finally, we show that the optimal pulse is robust against atom number fluctuations.

DOI: 10.1103/PhysRevLett.106.190501

PACS numbers: 03.67.–a, 05.10.–a

Classical control theory has played a major role in the development of present-day technologies [1]. Likewise, recently developed quantum optimal control methods [2–4] can be applied to emerging quantum technologies, e.g., quantum information processing—until now, at the level of a few qubits [5–7]. However, such methods encounter severe limits when applied to many-body quantum systems: due to the complexity of simulating the latter, existing quantum control algorithms (requiring many iterations to converge) usually fail to yield a desired final state within an acceptable computational time. A paradigmatic application of control of a many-body quantum system is the control of the dynamics of a quantum phase transition. The process of crossing a phase transition in an optimal way has been studied for decades for classical systems. Only recently it has been recast in the quantum domain, attracting a lot of attention (see, e.g., [8] and references therein) since, for instance, it has implications for adiabatic quantum computation and quantum annealing [9]. A transition between different phases is usually performed by “slowly” (adiabatically) sweeping an external control parameter across the critical point, allowing for a transformation from the initial to the final system ground state with sufficiently high probability. However, at the critical point in the thermodynamical limit a perfect adiabatic process is forbidden in finite time [10]. Thus, the resulting final state (for finite-time transformations) is characterized by some residual excitation energy, corresponding to the formation of topological defects within finite-size domains. The Kibble-Zurek theory has been shown to yield good estimates of the density of defects or of the residual energy [8,11]. The importance of these estimates in the quantum domain is underscored by the fact that, apart from very specific cases where analytical solutions are available, theoretical investigations must rely on heavy numerical

simulations due to the exponential growth of the Hilbert space with the system size and to the diverging entanglement at the critical point [12]. Nevertheless, it is possible to perform one-dimensional simulations of the dynamics by means of tensor-network-based techniques such as the time-dependent density matrix renormalization group (tDMRG) [13].

The basic underlying idea of classical control is to pick a specific path in parameter space to perform a specific task. This is formally a cost functional extremization that depends on the state of the system and is attained by varying some external control parameters. In a quantum-mechanical context, a big advantage is that the goal can be reached via interference of many different paths in parameter space, rather than just one. In few-body quantum systems, it has been shown that optimal control finds optimal paths in the parameter space that result in constructive interference of the system’s classical trajectories toward a given goal [4]. Indeed, present optimal control strategies demonstrated an impressive control of quantum systems, ranging from optimization of NMR pulses [7] to atomic [14] and superconducting qubits [5], as well as the crossing of a quantum phase transition in the analytically solvable quantum Ising model [15]. However, despite their effectiveness, they cannot be efficiently applied to systems that require tensor network methods for their simulation.

This Letter marks a step further—it provides for the first time a means to control the evolution of a nonintegrable many-body quantum system, resulting in the optimization of a given figure of merit. This is done by introducing a strategy to integrate optimal control with tDMRG simulations of the many-body quantum dynamics.

*Tensor-network-simulations.*—Tensor network methods are based on the assumption that it is possible to describe approximately a wide class of states with a simple tensor

structure. In particular the DMRG describes ground state static properties of one-dimensional systems by means of a matrix product state (MPS) [16]. The main characteristic of a MPS is that the resources needed to describe a given system depend only polynomially on the system size  $N$ , due to the introduction of an ancillary dimension  $m$  that determines the precision of the approximation. Since an exact description requires exponentially increasing resources with the number of components  $N$ , the tensor network approach results in an exponential gain in resources. Given a system Hamiltonian, the best possible approximated description of the system ground state—within the MPS at fixed  $m$ —is determined by means of an efficient energy minimization. With some slight modification, discretizing the time  $T = n_{\text{steps}} \Delta t$  and performing a Trotter expansion, the algorithm can be adapted to follow a state time evolution, the so-called tDMRG [13]. The tDMRG is a very powerful numerical method for efficiently numerically simulating the time evolution of one-dimensional many-body quantum systems. The class of states and of time evolutions that can be efficiently described with a small error are determined by the presence of entanglement between the different system components [12]. Here, we will use the tDMRG for the simulation of cold atoms in time-dependent optical lattices, which we feed into the chopped random basis (CRAB) optimization algorithm as described below.

*CRAB method.*—The general scenario of an optimal control problem can be stated as follows: given a system described by a Hamiltonian  $H$  depending on some control parameters  $c_j(t)$  with  $j = 1, \dots, N_C$ , the goal is to find the  $c_j$ 's time dependence (pulse shape) that extremizes a given figure of merit  $\mathcal{F}$ , for instance, the final system energy, state fidelity, or entanglement. We then start with an initial pulse guess  $c_j^0(t)$  and look for the best correction that has a simple expression in a given functional basis. As an explicative example, here we focus on the case where the correction is of the form  $c_j(t) = c_j^0(t)f_j(t)$ , and the functions  $f_j(t)$  can be simply expressed in a truncated Fourier space, depending on the expansion coefficients  $\vec{a}_j = a_j^k$  ( $k = 1, \dots, M_j$ ). In particular, in the following, we start from an initial ansatz, e.g., an exponential or linear ramp, and we introduce a correction of the form

$$f(t) = \frac{1}{\mathcal{N}} \left[ 1 + \sum_k A_k \sin(\nu_k t) + B_k \cos(\nu_k t) \right]. \quad (1)$$

Here,  $k = 1, \dots, M$ ,  $\nu_k = 2\pi k(1 + r_k)/T$  are “randomized” Fourier harmonics,  $T$  is the total time evolution,  $r_k \in [0:1]$  are random numbers with a flat distribution, and  $\mathcal{N}$  is a normalization constant to keep the initial and final control pulse values fixed. The optimization problem is then reformulated as the extremization of a multivariable function  $\mathcal{F}(\{A_k\}, \{B_k\}, \{\nu_k\})$ , which can be numerically approached with a suitable method, e.g., steepest descent or conjugate gradient [17]. When using CRAB together

with tDMRG, computing the gradient of  $\mathcal{F}$  is extremely resource consuming, if not impossible. Thus we resort to a direct search method like the Nelder-Mead or Simplex methods [17]. They are based on the construction of a polytope defined by some initial set of points in the space of parameters that “rolls down the hill” following predefined rules until reaching a (possibly local) minimum (see Fig. 1). Because of the fact that direct search methods are based on many *independent* evaluations of the function to be minimized, they can be efficiently implemented together with tDMRG simulations (and possibly performed in parallel). We stress that the functional dependency of the correction presented here [Eq. (1)] is one possible approach: different strategies might be explored. Indeed, making a given choice confines the search of the optimal driving field in a subspace of the whole space of functions and the results might depend on this choice. On the other hand, this approach simplifies the optimization problem that would be otherwise computationally unfeasible when tDMRG simulations are needed. As shown below, the described choice allows us to perform a successful optimization.

*Optical-lattice system.*—Very recently, the experimental and theoretical analysis of the dynamics of cold atoms in optical lattices has experienced a fast development, after the experimental demonstration of coherent manipulation of ultracold atoms in the seminal work of Ref. [18], where a Bose-Einstein condensate is first loaded into a single trap, and then a periodic lattice potential is slowly ramped up, inducing a quantum phase transition to a Mott insulator. This is the enabling step for a wide range of experiments, from transport or spectroscopy to quantum information processing [19]. In most of these applications, it is essential to achieve the lowest possible number of defects in the final state, that is, to reach exactly a final state with fixed number of atoms per site, e.g., unit filling. Up to now, this has been pursued by limiting the process speed—the superfluid-Mott insulator transition has been performed in about a hundred milliseconds, with a density of defects typically of the order of 10% [20].

Cold atoms in an optical lattice can be described by the Bose-Hubbard model defined by the Hamiltonian [19,21]

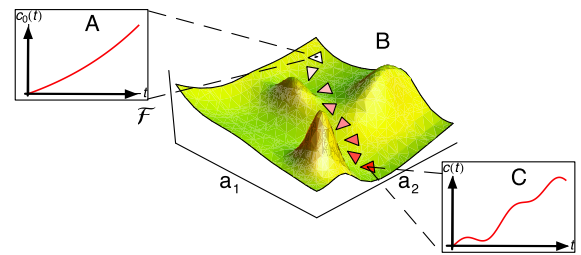


FIG. 1 (color online). (a) An initial guess pulse  $c^0(t)$  is used as a starting point. (b) The function  $\mathcal{F}(\vec{a})$  for the case  $\vec{a} = \{a_1, a_2\}$  and the initial polytope (white triangle) are defined and moved “downhill” [darker gray (red) triangles] until convergence is reached. (c) The final point is recast as the optimal pulse  $c(t)$ .

$$H = \sum_j \left[ -J(b_j^\dagger b_{j+1} + \text{H.c.}) + \Omega \left( j - \frac{N}{2} \right)^2 n_j + \frac{U}{2} (n_j^2 - n_j) \right]. \quad (2)$$

The first term on the right-hand side of Eq. (2) describes the tunneling of bosons between neighboring sites with rate  $J$ ;  $\Omega$  is the curvature of the external trapping potential, and  $n_j = b_j^\dagger b_j$  is the density operator with bosonic creation (annihilation) operators  $b_j^\dagger$  ( $b_j$ ) at site  $j = 1, \dots, N$ . The last term is the on-site contact interaction with energy  $U$ . The system parameters  $U$  and  $J$  can be expressed as a function of the optical-lattice depth  $V$  (we set  $\hbar = 1$  from now on) [19]. As sketched in Fig. 2, the system undergoes a quantum phase transition from a superfluid phase to a Mott insulator as a function of the ratio  $J/U$ . In a homogeneous one-dimensional system, the quantum phase transition is expected to occur at  $J_c/U \approx 0.083$ , where (upon decreasing the ratio  $J/U$ ) the ground state wave function drastically changes from a Fermi-Thomas distribution with high fluctuations in the number of particles per site to a simple product of local Fock states with no fluctuations in the number of atoms per site [19]. In the presence of an external trapping potential on top of the optical lattice, the phase diagram is more complex: the two phases coexists in different trap regions and typical “cake” structures are formed [22].

**Results.**—Following previous numerical studies [23] that modeled the experiment [24], and supported by strong evidence of agreement between numerical simulations and experimental results [25,26], we studied both the ideal homogeneous system ( $\Omega = 0$ ) and the experimental setup of [25] where the trapping potential is present. We applied the CRAB optimization to the preparation of a Mott insulator with ultracold atoms in an optical lattice; that is, we optimized the ratio  $J/U(t)$  that drives the superfluid-Mott

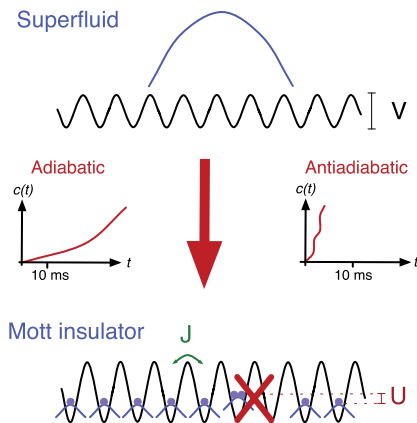


FIG. 2 (color online). Scheme of the Mott-superfluid transition in the homogeneous system for average occupation number  $\langle n \rangle = 1$ : increasing the lattice depth  $V$  (black line) the atom’s superfluid wave functions (upper) localize in the wells (lower). If the transition is not adiabatic—or optimized—defects appear (here represented by a hole and a doubly occupied site).

insulator transition. The resulting optimal ramp shape drives the system into a final Mott insulator state with a density of defects below half a percent in a total time of the order of a few milliseconds, amounting to a drastic improvement in the process time and in the quality of the final state—by about 2 orders of magnitude and by more than 1, respectively.

We consider a starting value of the lattice depth  $V(0) = 2E_r$  corresponding to  $J/U(0) \sim 0.52$ , since the description of the experimental system by Eq. (2) breaks down for  $V(0) \lesssim 2E_r$  [21]. However, the initial lattice switching on ( $V = 0 \rightarrow 2E_r$ ) can be performed very quickly without exciting the system (few milliseconds at most) [27]. We optimize the ramp to obtain the minimal residual energy per site  $\Delta E/N = (E(T) - E_G)/N$  (where  $E_G$  is the exact final ground state energy). In all simulations performed we set the total time  $T = 50\hbar/U \approx 3.01$  ms and the final lattice depth  $V(T)/E_r = 22 \sim 2.4 \times 10^{-3} J/U$ , deep inside the Mott insulator phase. Unless explicitly stated, we set the average occupation to one ( $\sum_i \langle n_i \rangle = N$ ). In all DMRG simulations, we exploited the conservation of the number of particles and used  $m = 20, \dots, 100$ ,  $\Delta t = 10^{-2} - 10^{-3}$ . We computed the final density of defects  $\rho = \frac{1}{N} \sum_i |\langle n_i \rangle - 1|$ : when it reached a given threshold  $\rho_c = 10^{-3}$ , the optimization was halted. In Fig. 3 we report a typical result of the optimization process: the initial guess and final optimal ramp for the system in the presence of the confining trap are shown for the parameter values corresponding to the experiment [24], for a system size  $N = 30$ . As can be clearly seen, the pulse is modulated with respect to the initial exponential guess and no high frequencies are present, reflecting the constraint introduced by the CRAB optimization. In the inset we display the final occupation numbers and the corresponding fluctuations, for the initial exponential ramp and the optimal pulse in the case

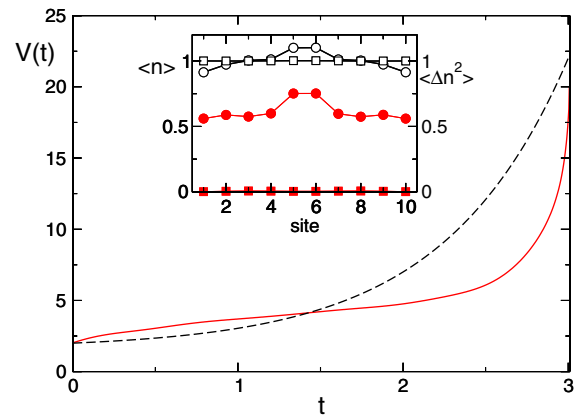


FIG. 3 (color online). Initial guess (dashed black line) and optimal ramp (solid red line)  $V(t)$  for the Bose-Hubbard model in the presence of the trap with  $N = 30$  sites, total time evolution  $T \approx 3$  ms. Inset: Populations  $\langle n_i \rangle$  (empty black symbols) and fluctuations  $\langle \Delta n_i^2 \rangle$  (full red symbols) at time  $t = T$  for the exponential initial guess (circles) and optimal ramp (squares) for  $N = 10$ .

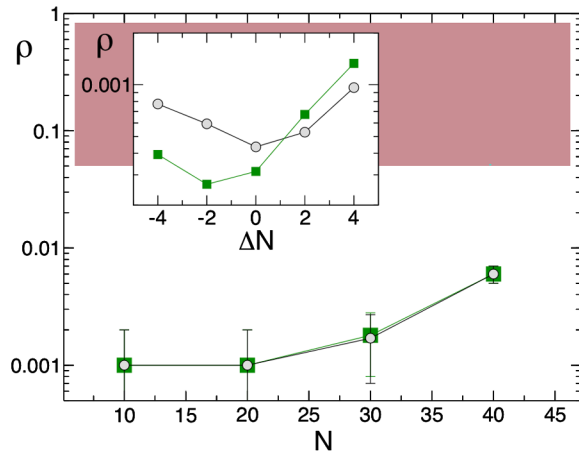


FIG. 4 (color online). Residual defect density  $\rho$  for  $N = 10, 20, 30, 40$ ,  $T \approx 3$  ms,  $\rho_c = 0.001$  for the homogeneous system (green squares) and in the presence of the trap (gray circles). The gray (red) region highlights the typical  $\rho$  for different initial ramp shapes (see text). Inset: Final  $\rho$  computed applying the pulse optimized for system size  $N = 20$  to different system sizes  $\Delta N = -4, \dots, 4$  (at constant filling). The results are almost independent from the truncation error for  $m > 50$ .

$N = 10$ . The figure clearly demonstrates the convergence to a Mott insulator in the latter case as fluctuations are drastically reduced and the occupation is exactly one for every site.

Finally, in Fig. 4 we plot the optimized density of defects  $\rho$  as a function of the system size (up to  $N = 40$ ) for the homogeneous and for the trapped system, demonstrating an improvement with respect to the initial guess by 1 (2) orders of magnitudes. Indeed, the exponential guess—like other guesses: linear, random, and a pulse optimized for a smaller system ( $N = 8$  sites)—gave residual density of defects of the order of 10% [gray (red) region in Fig. 4]. To check the experimental feasibility of our findings, we studied the stability of the optimal evolutions under different sources of error and experimental uncertainties, like atom number fluctuations. The inset of Fig. 4 shows the final density of defects when an optimal pulse computed for a given system size is applied to a different system size (keeping the average filling constant). As can be seen, the optimization works also for system size fluctuations of up to 20%: the final density of defects is of the same order. This robustness is crucial as the experimental realization of these systems is performed in parallel on many different one-dimensional tubes with different numbers of atoms [19]. We also checked the cases of different filling and of pulse distortion obtaining similar results (data not shown).

*Outlook.*—In conclusion, we would like to mention that the CRAB optimization strategy introduced here can in principle be applied also to open quantum many-body systems, e.g., by means of recently introduced numerical techniques [28]. Perhaps an even more stimulating perspective would be that of implementing it with a quantum system in place of the tDMRG classical simulator,

i.e., performing a CRAB-based closed-loop optimization [29]. The optimization might be performed during the experimental repetitions of the measurement processes, thus adding a small overhead to the experimental complexity. This would extend the applicability of the CRAB method to the optimization of quantum phenomena that are completely out of reach for simulation on classical computers, and represent a major design tool for future quantum technologies.

We thank F. Dalfovo, J. Denschlag, R. Fazio, C. Fort, M. Greiner, C. Koch, C. Menotti, G. Pupillo, and M. Rizzi for discussions, and the PwP project [30], the DFG (SFB/TRR 21), the bwGRiD, and the EC (Grant No. 247687, AQUTE, and PICC) for support.

\*simone.montangero@uni-ulm.de

- [1] J. T. Betts, *Practical Methods for Optimal Control Using Nonlinear Programming* (SIAM, Philadelphia, 2001).
- [2] D. D'Alessandro, *Introduction to Quantum Control and Dynamics* (Chapman & Hall/CRC, London, 2007).
- [3] C. Brif, R. Chakrabarti, and H. Rabitz, arXiv:0912.5121.
- [4] V. F. Krotov, *Global Methods in Optimal Control Theory* (Marcel Dekker, New York, 1996).
- [5] S. Montangero, T. Calarco, and R. Fazio, *Phys. Rev. Lett.* **99**, 170501 (2007).
- [6] P. Reberntrost *et al.*, *Phys. Rev. Lett.* **102**, 090401 (2009).
- [7] N. Khaneja *et al.*, *J. Magn. Reson.* **172**, 296 (2005).
- [8] W. H. Zurek, U. Dorner, and P. Zoller, *Phys. Rev. Lett.* **95**, 105701 (2005).
- [9] E. Farhi *et al.*, *Science* **292**, 472 (2001).
- [10] M. Born and V. A. Fock, *Z. Phys.* **51**, 165 (1928).
- [11] W. H. Zurek, *Phys. Rep.* **276**, 177 (1996).
- [12] G. Vidal, *Phys. Rev. Lett.* **91**, 147902 (2003).
- [13] U. Schollwöck, *Rev. Mod. Phys.* **77**, 259 (2005).
- [14] T. Calarco *et al.*, *Phys. Rev. A* **70**, 012306 (2004).
- [15] T. Caneva *et al.*, arXiv:1011.6634.
- [16] S. Östlund and S. Rommer, *Phys. Rev. Lett.* **75**, 3537 (1995); J. I. Cirac and F. Verstraete, *J. Phys. A* **42**, 504004 (2009).
- [17] W. H. Press *et al.*, *Numerical Recipes* (Cambridge University Press, New York, 2007).
- [18] M. Greiner *et al.*, *Nature (London)* **415**, 39 (2002).
- [19] I. Bloch, J. Dalibard, and W. Zwerger, *Rev. Mod. Phys.* **80**, 885 (2008).
- [20] D. Jaksch and P. Zoller, *Ann. Phys. (N.Y.)* **315**, 52 (2005).
- [21] D. Jaksch *et al.*, *Phys. Rev. Lett.* **81**, 3108 (1998).
- [22] G. G. Batrouni *et al.*, *Phys. Rev. Lett.* **89**, 117203 (2002).
- [23] C. Kollath *et al.*, *Phys. Rev. Lett.* **97**, 050402 (2006).
- [24] T. Stöferle *et al.*, *Phys. Rev. Lett.* **92**, 130403 (2004).
- [25] C. D. Fertig *et al.*, *Phys. Rev. Lett.* **94**, 120403 (2005).
- [26] I. Danshita and C. W. Clark, *Phys. Rev. Lett.* **102**, 030407 (2009).
- [27] M. Greiner (private communication).
- [28] M. Zwolak and G. Vidal, *Phys. Rev. Lett.* **93**, 207205 (2004).
- [29] C. Brif, R. Chakrabarti, and H. Rabitz, *New J. Phys.* **12**, 075008 (2010).
- [30] www.dmrq.it